
Exploiting Phonological Similarities between African Languages to achieve Speech to Speech Translation

Peter Ochieng, Dennis Kaburu

Abstract

This paper presents a pilot study on direct speech-to-speech translation (S2ST) by leveraging linguistic similarities among selected African languages within the same phylum, particularly in cases where traditional data annotation is expensive or impractical. We propose a segment-based model that maps speech segments both within and across language phyla, effectively eliminating the need for large paired datasets. By utilizing paired segments and guided diffusion, our model enables translation between any two languages in the dataset. We evaluate the model on a proprietary dataset from the Kenya Broadcasting Corporation (KBC), which includes five languages: Swahili, Luo, Kikuyu, Nandi, and English. The model demonstrates competitive performance in segment pairing and translation quality, particularly for languages within the same phylum. Our experiments reveal that segment length significantly influences translation accuracy, with average-length segments yielding the highest pairing quality. Comparative analyses with traditional cascaded ASR-MT techniques show that the proposed model delivers nearly comparable translation performance. This study underscores the potential of exploiting linguistic similarities within language groups to perform efficient S2ST, especially in low-resource language contexts.

1 Introduction

To facilitate communication between people who do not share a common language, the machine learning community has proposed techniques for speech-to-speech translation (S2ST), which converts speech from one language to another. The standard approach typically involves three key sub-tasks: automatic speech recognition (ASR), text-to-text translation, and text-to-speech (TTS) synthesis Ney (1999); Matusov et al. (2005); Vidal (1997).

Although this cascaded approach has achieved some success, it has also been criticized due to error propagation. Errors in one sub-task are compounded in subsequent tasks, leading to increased translation inaccuracies. Furthermore, while the cascaded process captures the semantics of the original speech, important speech elements such as the speaker’s unique characteristics (indexical components) and the natural rhythm of communication are often lost during translation Barrault et al. (2023b). These components are crucial in many social and conversational contexts.

For low-resource languages, such as African languages, the cascaded approach faces additional challenges. The lack of aligned or annotated text between languages makes text-to-text translation difficult or impossible in some cases. In response to these issues, researchers have started exploring direct S2ST, which bypasses the need for intermediate text-based representations.

Implementing direct S2ST remains challenging due to the lack of sufficient annotated speech pairs needed for fully supervised end-to-end training Jia et al. (2019). Collecting and annotating speech datasets is significantly more difficult than gathering parallel text pairs used in the cascaded approach. This challenge has motivated innovative solutions from various works Jia et al. (2019); Zhang et al. (2021); Jia et al. (2021); Lee et al. (2021); Huang et al. (2022), which leverage deep neural networks to perform direct S2ST without requiring parallel speech datasets.

While prior works on direct S2ST have shown promising results using deep learning models, our approach differentiates itself by explicitly leveraging linguistic relationships among languages within the same phylum to improve speech segment annotation. We introduce two segment-mapping techniques that capitalize on phonological similarities across related languages, which prior methods have not explored in this context.

Guided diffusion is a generative modeling technique that iteratively refines a noisy input toward a target distribution. In the context of S2ST, we adapt this model to speech data, using a pseudo-classifier trained on paired segments to guide the diffusion process. This enables us to generate clean speech segments in the target language using paired segments of speech.

To evaluate our technique, we conduct a pilot study using selected African languages. These languages are categorized into four major phyla: Niger-Congo, Nilo-Saharan, Afroasiatic, and Khoisan Childs (2003); Frajzyngier (2018). We assess the efficacy of segment-mapping techniques by testing on languages within the same phylum and across different phyla to understand how phonological relationships impact translation performance.

Given two speeches in languages x and y , both conveying the same semantic content, we investigate whether the speech segments in x , extracted using silences, can be directly mapped to segments in y , particularly when both languages belong to the same phylum. We also examine whether the mapping quality deteriorates when y is from a different phylum.

We propose two segment-mapping techniques: one based on the similarity of segment locations within the speech and the other based on the similarity of learned embeddings through contrastive training. By automating speech segment mapping, we aim to reduce the manual effort and cost involved in annotating speech datasets. Once the segments are aligned, we employ a guided diffusion model to train a direct S2ST system. Our contributions are as follows:

1. Investigate the extent to which linguistic similarities within a phylum can be leveraged for automatic speech segment annotation, offering a scalable solution for low-resource languages.
2. Explore the feasibility of automatic speech segment annotation across languages from different phyla, contributing to cross-lingual translation tasks.
3. Propose two techniques for segment alignment—location-based and embedding-based techniques.
4. Develop an automatic evaluation method for segment pairing, minimizing reliance on costly human evaluations and enabling more scalable annotation efforts.
5. Introduce a direct S2ST model using guided diffusion.

2 Background

2.1 Guided diffusion

Guided diffusion involves learning the conditional distribution $p(x|y)$. Guidance therefore involves learning the conditional distribution which enables the model to generate the data x by conditioning it on information y . Using Tweedie’s formula which states that the true mean of samples drawn from an exponential family distribution can be estimated using the maximum likelihood estimate of the samples plus the correcting term involving the score of the estimate, the mean of the distribution $z \sim \mathcal{N}(z; u_z, \Sigma)$ can be estimated as:

$$\mathbb{E}(u_z|z) = z + \Sigma \nabla_z \log p(z) \tag{1}$$

Therefore, given the posterior $q(x_t|x_0) = \mathcal{N}(x_t; \sqrt{\bar{\alpha}_t}x_0, (1 - \bar{\alpha}_t)I)$, its true mean is estimated as:

$$\mathbb{E}(u_{x_t}|x_t) = x_t + (1 - \bar{\alpha}_t) \nabla_{x_t} \log p(x_t) \tag{2}$$

Where $\bar{\alpha}_t = \prod_{i=1}^t \alpha_i$, $\epsilon_0 \sim \mathcal{N}(\epsilon_0; 0, I)$ and α_t evolves with time t based on a fixed or learnable schedule such that the final distribution $p(x_T)$ is a standard Gaussian. Hence:

$$\sqrt{\bar{\alpha}_t}x_0 = x_t + (1 - \bar{\alpha}_t) \nabla_{x_t} \log p(x_t) \tag{3}$$

$$x_0 = \frac{x_t + (1 - \bar{\alpha}_t)\nabla_{x_t} \log p(x_t)}{\sqrt{\bar{\alpha}_t}} \quad (4)$$

Using the property of isotropic Gaussians, Ho et al. (2020) show that x_t can be derived directly on x_0 and therefore,

$$x_0 = \frac{x_t - \sqrt{1 - \bar{\alpha}_t}\epsilon_\theta(x_t, t)}{\sqrt{\bar{\alpha}_t}} \quad (5)$$

Equating equation 4 and 5,

$$\nabla_{x_t} \log p(x_t) = -\frac{1}{\sqrt{1 - \bar{\alpha}_t}}\epsilon_\theta(x_t, t) \quad (6)$$

The conditional model score $\nabla_{x_t} \log p(x_t|y)$ at an arbitrary noise level t can be expressed as:

$$\begin{aligned} \nabla_{x_t} \log p(x_t|y) &= \nabla_{x_t} \log\left(\frac{p(x_t)p(y|x_t)}{p(y)}\right) = \nabla_{x_t} \log p(x_t) + \nabla_{x_t} \log p(y|x_t) - \nabla_{x_t} \log p(y) = \\ &\nabla_{x_t} \log p(x_t) + \nabla_{x_t} \log p(y|x_t) \end{aligned} \quad (7)$$

Replacing $\nabla_{x_t} \log p(x_t)$ according to equation 6 in equation 7 we have:

$$\nabla_{x_t} \log p(x_t|y) = \nabla_{x_t} \log p(x_t) + \nabla_{x_t} \log p(y|x_t) = -\frac{1}{\sqrt{1 - \bar{\alpha}_t}}\epsilon_\theta(x_t, t) + \nabla_{x_t} \log p(y|x_t) \quad (8)$$

$$-\sqrt{1 - \bar{\alpha}_t}\nabla_{x_t} \log p(x_t|y) = \epsilon_\theta(x_t, t) - \sqrt{1 - \bar{\alpha}_t}\nabla_{x_t} \log p(y|x_t) \quad (9)$$

$$\hat{\epsilon}(x_t, t) := \epsilon_\theta(x_t, t) - \sqrt{1 - \bar{\alpha}_t}\nabla_{x_t} \log p(y|x_t) \quad (10)$$

Equation 10 can be plugged in the sampling process of a pre-trained diffusion model to guide sample generation. DDPM based diffusion models have been criticised for being slow in sample generation since they require many steps. To remedy this, work in Song et al. (2020) proposes Denoising Diffusion Implicit Models (DDIM) which are non-Markovian diffusion based models that use sampling process defined in equation 11 to generate samples from a pre-trained DDPM model $\epsilon_\theta(x_t, t)$.

$$x_{t-1} := \sqrt{\bar{\alpha}_{t-1}}\left(\frac{x_t - \sqrt{1 - \bar{\alpha}_t}\epsilon_\theta(x_t, t)}{\sqrt{\bar{\alpha}_t}}\right) + \sqrt{1 - \bar{\alpha}_{t-1} - \sigma_t^2}\epsilon_\theta(x_t, t) + \sigma_t\epsilon_t \quad (11)$$

where $\epsilon_t \sim \mathcal{N}(\epsilon_t; 0, I)$. The sampling process based on equation 11 allows using different samplers by changing the variance noise σ_t . When $\sigma_t = 0$, DDIM sampling becomes deterministic since it allows for full inversion of the latent variable into original input. The inversion can be achieved using significantly fewer steps than those used in the forward process of the pre-trained DDPM. This significantly accelerates sample generation. The modified error $\hat{\epsilon}(x_t, t)$ derived in equation 10 can be plugged directly in DDIM sampling in equation 11 as follows:

$$x_{t-1} := \sqrt{\bar{\alpha}_{t-1}}\left(\frac{x_t - \sqrt{1 - \bar{\alpha}_t}\hat{\epsilon}(x_t, t)}{\sqrt{\bar{\alpha}_t}}\right) + \sqrt{1 - \bar{\alpha}_{t-1}} \quad (12)$$

In equation 12 we set $\sigma_t = 0$.

3 Related work

To facilitate communication between people who do not share common language, machine learning community have proposed techniques that implement speech-to-speech translation (S2ST) which entails translating speech from one language to another. The de-facto way of implementing S2ST is to break the process into three key sub-tasks i.e., automatic speech recognition, text-to-text translation, and text-to-speech synthesis Ney (1999) Matusov et al. (2005) Vidal (1997). Even though this cascaded approach has achieved some level of success in S2ST, it has been criticised due to the fact that errors made at a given sub-task are compounded in subsequent tasks leading to larger translation errors. Further, when speech is translated in this manner even when translation can accurately capture the semantics of the original speech, certain key elements of the original speech are lost in the translation process Schuller et al. (2013). Elements of speech

such as characteristics of the speaker (referred to as indexical component) and the natural way commutation is carried out in a social setting are lost Barrault et al. (2023b). For Low resource languages such as African languages, the use of cascaded approach to achieve S2ST faces an additional problem of lack of aligned or annotated text between languages making text-to-text translation sometimes impossible to achieve. Due to these issues with cascaded S2ST, researchers have explored the implementation of direct S2ST. Implementing direct S2ST solution is still a challenge due to lack of sufficient annotated speech pair to allow models to be trained in fully supervised end-to-end way Jia et al. (2019). This is due to the fact that collecting and annotating speech dataset is more challenging compared to collecting parallel text pairs used in cascaded approach Jia et al. (2019). This difficulty has made some works such as Jia et al. (2019), Zhang et al. (2021), Jia et al. (2021), Lee et al. (2021) and Huang et al. (2022) to design innovative ways that exploit deep neural network to train models that perform direct S2ST without the need for parallel speech dataset.

4 Direct S2ST based speech segmentation and guided diffusion

4.1 Speech segmentation

Speech segmentation is crucial in our proposed technique. We hypothesize that two speeches with the same semantic content and belonging to the same language phylum will have silences at approximately the same locations due to phonological similarities such as rhythm and prosody. These silences are leveraged to segment audio files into coherent sentences. Silence-based audio segmentation using voice activity detection (VAD) has been explored in previous studies Gaido et al. (2021); Potapczyk & Przybysz (2020); Duquenne et al. (2021). Although effective, VAD-based segmentation presents two key challenges.

One challenge is that pauses within a sentence may lead to incomplete or incoherent segments. Another issue is that pause-based segmentation can result in "spillover" sentences, where consecutive sentences are incorrectly grouped into one when no pause exists between them. To address these issues, over-segmentation techniques have been proposed in works such as Potapczyk & Przybysz (2020); Duquenne et al. (2021), which divide audio files more densely based on silence.

For example, Potapczyk & Przybysz (2020) defines a sentence threshold after dense segmentation, merging smaller fragments until they meet the threshold. Similarly, Duquenne et al. (2021) introduces an over-segmentation approach where segments must be at least 3 seconds and no more than 20 seconds long. While this increases recall, it comes at the cost of additional computation Barrault et al. (2023a).

In our approach, we adopt the technique from Duquenne et al. (2021), as experimental results showed it to be more robust and better suited for the speeches used in our evaluation, particularly for African languages. Given a speech x that contains multiple sentences, we apply a VAD tool to identify all silences within the input speech. These silences are used to extract segments, where each segment s_x is bounded by two silence timestamps and must be between 3 and 20 seconds in length.

4.2 Segment pairing

We propose a two-step process to pair segments from two speeches x and y , both containing similar semantic content. The first step pairs segments based on location, and the second step refines these pairs using contrastive self-supervised learning to filter out less accurate matches.

1. Segment both speeches x and y using the method described in Section 3.1.
2. Calculate the average segment lengths l_x and l_y , and determine the absolute difference $d = |l_x - l_y|$ to account for timing variations.
3. For each segment s_x of length p_x in speech x , find matching segments s_{y_i} in speech y within the length range $p_x \pm d$, and located between $i - d/2$ and $i + p_x + d/2$, accounting for variations in delivery speed.
4. If no match exists in speech y , generate overlapping segments from y with overlaps of $d/2$, and create all possible pairings.

-
- Reverse the process by mapping segments of y to those of x , ensuring bi-directional alignment.

This location-based alignment creates multiple one-to-many pairings, which are refined into one-to-one pairings using contrastive self-supervised learning.

4.2.1 Refinement with contrastive learning

To filter and select high-quality segment pairs, we train a segment encoder f_s using contrastive self-supervised learning. The goal is to learn a mapping function $f_s : s_x \mapsto \mathbb{R}^d$, which transforms each segment s_x into a d -dimensional vector. We employ the SimCLR contrastive loss Chen et al. (2020), treating segments from the same language as positive pairs and segments from different languages as negative pairs:

$$\mathbb{E}_{s_x, s_x^+, s_y} \left[-\log \left(\frac{e^{f_s(s_x)^T f_s(s_x^+)}}{e^{f_s(s_x)^T f_s(s_x^+)} + \sum_{i=1}^{n-2} e^{f_s(s_x)^T f_s(s_{y_i})}} \right) \right]$$

This loss encourages similarity between positive pairs $f_s(s_x), f_s(s_x^+)$, while minimizing similarity with negative pairs $f_s(s_x), f_s(s_y^-)$. Once trained, the encoder f_s generates embeddings for all segments from both speeches x and y .

Final one-to-one pairings are established by calculating the cosine similarity between the embeddings of segments from both speeches. For each segment s_x , we select the segment s_y that maximizes the cosine similarity:

$$(s_x, s_y) = \arg \max_y \cos(f_s(s_x), f_s(s_y))$$

Low-quality matches are filtered by retaining only those pairs validated by contrastive learning. From the initial location-based pairings $\{(s_x, s_{y_1}), \dots, (s_x, s_{y_n})\}$, we keep only pairs confirmed by contrastive learning:

$$(s_x, s_{y_i}) = \{(s_x, s_{y_i}), \dots, (s_x, s_{y_n})\} \cap \{(s_x, s_{y_i})\}$$

If no valid pairs remain, we fall back to selecting the segment s_{y_i} with the highest cosine similarity score, ensuring the closest semantic match.

To train the segment encoder f_s , we start by encoding the input segment s_x using an input encoder f_i , which is implemented as a single convolutional layer as proposed in ?. This layer consists of 256 convolutional filters, each with a kernel size of 16 samples and a stride of 8 samples. The input to this layer is a speech segment in the time domain, $s_x \in \mathbb{R}^T$, and the output is a time-frequency representation akin to the Short-Time Fourier Transform (STFT), denoted as $s_{x_0} \in \mathbb{R}^{F \times T}$:

$$s_{x_0} = \text{ReLU}(\text{Conv1d}(s_x))$$

The output $s_{x_0} \in \mathbb{R}^{F \times T}$ from the input encoder f_i is then fed into the segment encoder f_s , where we use EfficientNet-B0 Tan & Le (2019), a lightweight and highly scalable convolutional neural network designed to efficiently handle 2D inputs. No modifications were made to the EfficientNet-B0 architecture, and global max pooling is applied in the final layer to produce an output embedding $h \in \mathbb{R}^{720}$.

The projection head, following EfficientNet-B0, consists of a fully connected feed-forward layer with 512 units. This is followed by Layer Normalization and a tanh activation function, which regularize the embedding space and ensure the output is in a suitable range for contrastive learning. The projection head maps the 720-dimensional embedding h from EfficientNet-B0 to a 512-dimensional latent space, used during contrastive training to facilitate the SimCLR loss. After training, the projection head is discarded, and only the output of EfficientNet-B0 is used as the final embedding for each segment.

4.3 Guided translation

Figure 1 illustrates the flow of the proposed guided translation method, comprising three main modules: the input encoder f_i , the pseudo-classifier, and the pre-trained diffusion model.

First, the input encoder converts paired speech segments s_x and s_y into their representations s_{x_0} and s_{y_0} . The target representation s_{x_0} , representing the latent form of the target speech, is transformed into its noisy version $s_{x_{t_x}}$, where t_x refers to the diffusion timestep of the target segment. This noising process follows the same forward diffusion process of the pre-trained diffusion model, with $t_x \sim \mathcal{U}(1, T)$.

Next, the noisy latent $s_{x_{t_x}}$, along with the clean source segment s_{y_0} , is passed to the pseudo-classifier, which computes $f(s_{x_{t_x}}) \cdot f(s_{y_0})$. This step aligns the noisy latent representation of the target speech $s_{x_{t_x}}$ at time t_x with the source speech s_{y_0} (at $t_y = 0$). The diffusion model then predicts the noise $\epsilon_\theta(s_{x_{t_x}}, t_x)$ present in $s_{x_{t_x}}$.

Finally, the predicted noise $\epsilon_\theta(s_{x_{t_x}}, t_x)$ and the pseudo-classifier output are used to estimate a modified noise $\hat{\epsilon}_\theta(s_{x_{t_x}}, t_x)$ (see Equation 10). This modified noise is input into the DDIM sampling process (Equation 12) to estimate $s_{x_{t_{x-1}}}$, refining the latent variable step-by-step. The estimated $s_{x_{t_{x-1}}}$ is further refined through subsequent steps in the DDIM sampling process until the final de-noised target speech segment s_{x_0} is generated. Further details are provided in the following section.

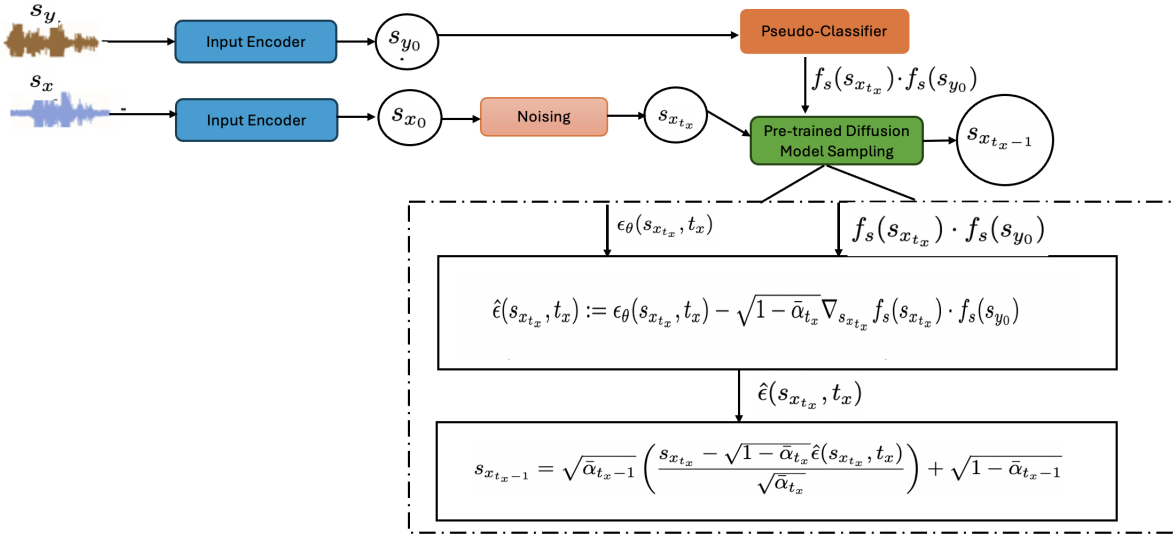


Figure 1: Overview of the proposed guided diffusion process for S2ST, showing the flow from the input encoder, through the pseudo-classifier, to the diffusion model and DDIM sampling.

4.3.1 Pseudo-classifier model

Inspired by CLIP Radford et al. (2021), which learns joint representations between text and images, we propose learning joint representations of speech segments from two different languages. Unlike CLIP, which uses two separate encoders for its multimodal inputs, our pseudo-classifier employs a single encoder—the segment encoder f_s —to generate representations of paired speech segments from languages x and y . The output of the pseudo-classifier is the dot product $f_s(s_x) \cdot f_s(s_y)$ between the representations of the paired segments, which measures their similarity.

Concretely, given paired speech segments (s_x, s_y) , we first use the input encoder f_i described in Section 4.3.1 to obtain intermediate representations $s_{x_0} \in \mathbb{R}^{F \times T}$ and $s_{y_0} \in \mathbb{R}^{F \times T}$, where $t_x = 0$ and $t_y = 0$ for clean representations. Noise is then injected into the target segment s_{x_0} , yielding $s_{x_{t_x}}$ at a later timestep t_x . Both $s_{x_{t_x}}$ and s_{y_0} are then passed through the segment encoder f_s . The output representations $f_s(s_{x_{t_x}})$ and

$f_s(s_{y_0})$ are combined via a dot product to generate the similarity score $f_s(s_{x_{t_x}}) \cdot f_s(s_{y_0})$, which is subsequently used to guide the sampling process in the pre-trained diffusion model.

4.3.2 Unconditional pre-trained diffusion sampling for S2ST

Inspired by Nichol et al. (2021), which replaces the classifier in guided diffusion with a CLIP model for text-to-image generation, we similarly replace the classifier $p(y|x_t)$ in our guided diffusion process. Specifically, we substitute $\log p(y|x_t)$ with a pseudo-classifier $f_s(s_{x_{t_x}}) \cdot f_s(s_{y_0})$, as described in Equation 13.

$$\hat{\epsilon}(s_{x_{t_x}}, t_x) := \epsilon_\theta(s_{x_{t_x}}, t_x) - \sqrt{1 - \bar{\alpha}_{t_x}} \nabla_{s_{x_{t_x}}} (f_s(s_{x_{t_x}}) \cdot f_s(s_{y_0})) \quad (13)$$

The pseudo-classifier $f_s(s_{x_{t_x}}) \cdot f_s(s_{y_0})$ is generated based on noised speech segments $s_{x_{t_x}}$ from the target language and clean (un-noised) segment s_{y_0} from language y . The term $\epsilon_\theta(s_{x_{t_x}}, t_x)$ refers to the pre-trained diffusion model.

By replacing $\log p(y|x_t)$ with the pseudo-classifier $f_s(s_{x_{t_x}}) \cdot f_s(s_{y_0})$, the diffusion process is guided to maintain semantic consistency between the two languages.

We also perform an ablation study making the pseudo-classifier generate $f_s(s_{x_0}) \cdot f_s(s_{y_0})$, i.e., the target segments are not noised. This allows us to investigate whether noising target segments provides any benefit in the guiding process. The modified guided diffusion is implemented as shown in Equation 14:

$$\hat{\epsilon}(s_{x_{t_x}}, t_x) := \epsilon_\theta(s_{x_{t_x}}, t_x) - \sqrt{1 - \bar{\alpha}_{t_x}} \nabla_{s_{x_{t_0}}} (f_s(s_{x_{t_0}}) \cdot f_s(s_{y_0})) \quad (14)$$

Once the modified noise $\hat{\epsilon}(s_{x_{t_x}}, t_x)$ is computed, it is passed through the DDIM sampling process to iteratively refine the latent speech representation.

4.3.3 Conditional Pre-trained Diffusion Sampling for S2ST

Equations 13 and 14 apply when the underlying diffusion model is unconditional, i.e., the pre-trained diffusion model is modeling $p(s_x)$. To implement guided diffusion when the pre-trained diffusion model is conditional, i.e., modeling $p(s_x | s_y)$, we modify Equations 13 and 14 as follows.

The updated form of Equation 13 is:

$$\hat{\epsilon}_\theta^x(s_{x_{t_x}}, s_{y_0}, t_x, t_y = 0) := \epsilon_\theta^x(s_{x_{t_x}}, s_{y_0}, t_x, t_y = 0) - \sqrt{1 - \bar{\alpha}_{t_x}} \nabla_{s_{x_{t_x}}} (f_s(s_{x_{t_x}}) \cdot f_s(s_{y_0})) \quad (15)$$

Here, the pre-trained diffusion model $\epsilon_\theta^x(s_{x_{t_x}}, s_{y_0}, t_x, t_y = 0)$ estimates the noise injected into $s_{x_{t_x}}$ when $s_{x_{t_x}}$ is conditioned on s_{y_0} .

Similarly, Equation 14 is modified to the following form (Equation 16):

$$\hat{\epsilon}_\theta^x(s_{x_{t_x}}, s_{y_{t_0}}, t_x, t_0) := \epsilon_\theta^x(s_{x_{t_x}}, s_{y_0}, t_x, t_y = 0) - \sqrt{1 - \bar{\alpha}_{t_x}} \nabla_{s_{x_{t_0}}} (f_s(s_{x_0}) \cdot f_s(s_{y_0})) \quad (16)$$

4.4 Unified diffusion pre-trained model

Instead of training separate diffusion models for unconditional and conditional sampling, we propose a unified diffusion model that can handle both distributions.

4.4.1 Background

The goal is to design a unified diffusion model capable of capturing distributions derived from the joint distribution $q(x_0, y_0)$, including:

- The marginal distributions $q(x_0)$ and $q(y_0)$,

- The conditional distributions $q(x_0|y_0)$ and $q(y_0|x_0)$,
- The joint distribution $q(x_0, y_0)$.

In diffusion models, the marginal distribution $q(x_0)$ is modeled as the conditional distribution of noise injected into the latent variable x_t , i.e., $E[\epsilon^x|x_t]$. Similarly, the conditional distribution $q(x_0|y_0)$ and the joint distribution $q(x_0, y_0)$ are modeled as $E[\epsilon^x|x_t, y_0]$ and $E[\epsilon^x, \epsilon^y|x_t, y_t]$, respectively.

These can be unified as $E[\epsilon^x, \epsilon^y|x_{t_x}, y_{t_y}]$ Bao et al. (2023), where t_x and t_y are potentially different timesteps, and x_{t_x} and y_{t_y} are their corresponding latents. By setting $t_y = T$, the model estimates the marginal $E[\epsilon^x|x_{t_x}]$, and by setting $t_y = 0$, the conditional distribution $E[\epsilon^x|x_{t_x}, y_0]$ is modeled. The joint distribution $q(x_0, y_0)$ is modeled by setting $t_x = t_y = t$.

A joint diffusion model for noise prediction $\epsilon_0(x_{t_x}, y_{t_y}, t_x, t_y)$ is trained to predict the noise ϵ^x and ϵ^y injected into x_{t_x} and y_{t_y} , using the following objective:

$$E_{x_0, y_0, \epsilon^x, \epsilon^y, t_x, t_y} \left\| \epsilon_0(x_{t_x}, y_{t_y}, t_x, t_y) - [\epsilon^x, \epsilon^y] \right\|_2^2 \quad (17)$$

where $[\epsilon^x, \epsilon^y]$ is the concatenation of ϵ^x and ϵ^y , both sampled from a standard Gaussian distribution $\mathcal{N}(0, I)$, and t_x and t_y are uniformly sampled from $\mathcal{U}(1, T)$.

4.4.2 Training and Sampling of the Unified Diffusion Model

The training process, as summarized in Figure 2, consists of two key stages:

We begin by encoding speech segments from languages x and y into low-dimensional latent embeddings, denoted as s_{x_0} and s_{y_0} , using a speech encoder f_s . This encoder extracts essential features from each speech signal. For the latent representation s_{x_0} , a pre-trained diffusion model applies noise, generating the noisy embedding $s_{x_{t_x}}$. Similarly, s_{y_0} is transformed into $s_{y_{t_y}}$ through a forward diffusion process. The noise injection can occur at different timesteps, meaning that t_x may not necessarily equal t_y .

Once the noisy embeddings $s_{x_{t_x}}$ and $s_{y_{t_y}}$ are generated, the next task is to predict the noise injected into both segments. This is achieved using a transformer-based noise prediction network that consists of 8 transformer blocks designed to capture temporal dependencies in the data.

We enhance the transformer’s capability by concatenating the acoustic features of both speech segments, denoted as $[c_x, c_y]$, which are derived from their respective Mel-spectrogram representations. These concatenated features provide additional context, improving the accuracy of noise prediction.

Each transformer block in the model consists of the following components: - Multi-head attention (MHA) mechanism to capture relationships across different time steps. - Feed-forward layers (FFW) to process the embeddings in a non-linear manner. - Layer normalization to stabilize training.

Each transformer block is followed by a normalization layer and a final embedding layer, which outputs the predicted noise for both segments, ϵ_0^x for the noisy embedding $s_{x_{t_x}}$ and ϵ_0^y for the noisy embedding $s_{y_{t_y}}$.

The model is trained to minimize the error in noise prediction. The objective function is formulated as:

$$E_{s_{x_0}, s_{y_0}, \epsilon^x, \epsilon^y, t_x, t_y} \left\| \epsilon_0(s_{x_{t_x}}, s_{y_{t_y}}, t_x, t_y) - [\epsilon^x, \epsilon^y] \right\|_2^2$$

where $[\epsilon^x, \epsilon^y]$ are noise values sampled independently from a standard Gaussian distribution, representing the ground truth noise injected into the latent representations $s_{x_{t_x}}$ and $s_{y_{t_y}}$ at timesteps t_x and t_y , respectively.

The training process is detailed in Algorithm 1:

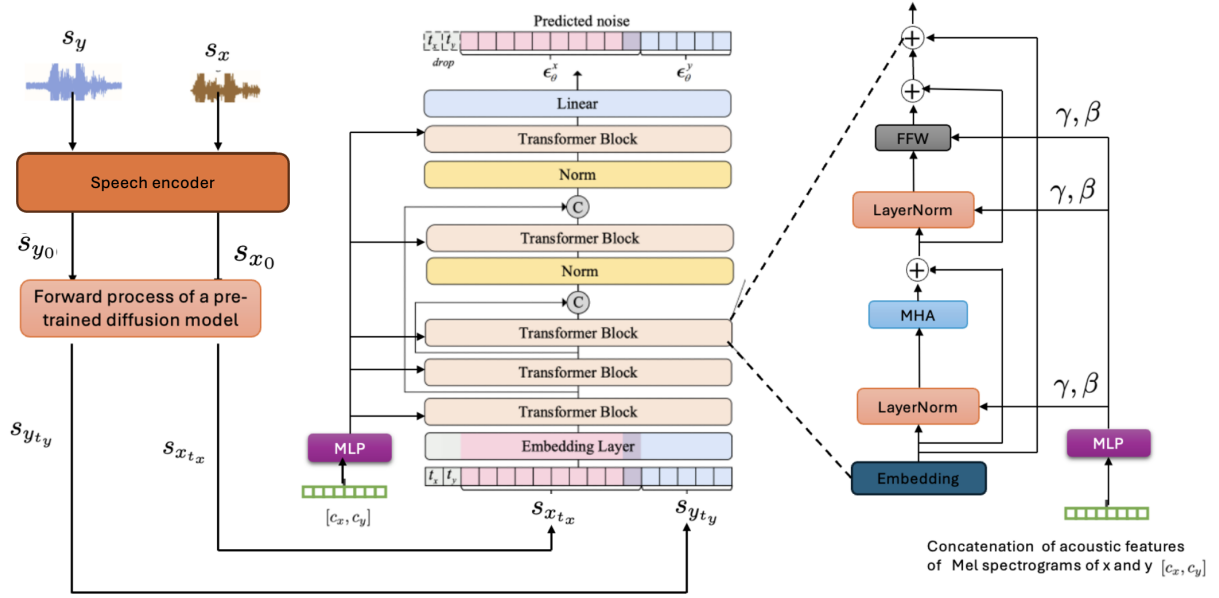


Figure 2: Overview of the guided diffusion process for speech-to-speech translation (S2ST). The input speech segments from the source (s_x) and target (s_y) languages are first processed by a speech encoder to generate latent embeddings (s_{x_0} and s_{y_0}). These embeddings are passed through a pre-trained diffusion model, which injects noise into the latent representations at different timesteps ($s_{x_{t_x}}$ and $s_{y_{t_y}}$). Acoustic features from the Mel-spectrograms of both speeches (c_x and c_y) are concatenated and processed by an MLP to provide additional context. The transformer-based noise prediction network, consisting of multiple transformer blocks with multi-head attention (MHA), feed-forward layers (FFW), and layer normalization, then predicts the injected noise (ϵ_x^t and ϵ_y^t) in both noisy segments.

Algorithm 1 Training

- 1: **repeat**
 - 2: $s_{x_0}, s_{y_0} \sim q(s_{x_0}, s_{y_0})$
 - 3: $t_x, t_y \sim \text{Uniform}(\{1, 2, \dots, T\})$
 - 4: $\epsilon^x, \epsilon^y \sim \mathcal{N}(0, I)$
 - 5: Let $s_{x_{t_x}} = \sqrt{\bar{\alpha}_{t_x}} s_{x_0} + \sqrt{1 - \bar{\alpha}_{t_x}} \epsilon^x$
 - 6: Let $s_{y_{t_y}} = \sqrt{\bar{\alpha}_{t_y}} s_{y_0} + \sqrt{1 - \bar{\alpha}_{t_y}} \epsilon^y$
 - 7: Take gradient step on $\nabla_{\theta} \|\epsilon_{\theta}(x_{t_x}, y_{t_y}, t_x, t_y) - [\epsilon^x, \epsilon^y]\|_2^2$
 - 8: **until** converged
-

Once training is complete, the model can be used to generate new speech segments. The sampling process differs depending on whether we are performing unconditional or conditional sampling.

In unconditional sampling (Algorithm 2), the target speech segment is generated from a noisy latent s_{x_T} without conditioning on a reference segment. In contrast, conditional sampling generates the target speech while conditioned on a reference segment s_{y_0} , guiding the generation to maintain semantic consistency with the reference.

Algorithm 2 Unconditional sampling of s_{x_0} given a diffusion model $\epsilon_\theta^x(s_{x_{t_x}}, s_{y_T}, t_x, t_y = T)$ and classifier $f(s_{x_{t_x}}) \cdot f(s_{y_0})$

```

1:  $s_{x_T} \sim \mathcal{N}(0, I)$ 
2: for  $t_x = T, \dots, 1$  do
3:    $\hat{\epsilon}_\theta^x(s_{x_{t_x}}, s_{x_T}, t_x, t_y = T) := \epsilon_\theta^x(s_{x_{t_x}}, s_{x_T}, t_x, t_y = T) - \sqrt{1 - \bar{\alpha}_{t_x}} \nabla_{s_{x_{t_x}}} f(s_{x_{t_x}}) \cdot f(s_{y_0})$ 
4:    $s_{x_{t_x-1}} := \sqrt{\bar{\alpha}_{t_x-1}} \left( \frac{s_{x_{t_x}} - \sqrt{1 - \bar{\alpha}_{t_x}} \hat{\epsilon}_\theta^x(s_{x_{t_x}}, s_{x_T}, t_x, t_y = T)}{\sqrt{\bar{\alpha}_{t_x}}} \right) + \sqrt{1 - \bar{\alpha}_{t_x-1}}$ 
5: end for
6: return  $s_{x_0}$ 

```

Algorithm 3 Sampling of $s_{x_{t_0}}$ conditioned on $s_{y_{t_0}}$

```

1:  $s_{x_T} \sim \mathcal{N}(0, I)$ 
2: for  $t_x = T, \dots, 1$  do
3:    $\hat{\epsilon}_\theta^x(s_{x_{t_x}}, s_{y_0}, t_x, t_y = 0) = \epsilon_\theta^x(s_{x_{t_x}}, s_{y_{t_y}}, t_x, t_y = 0) - \sqrt{1 - \bar{\alpha}_{t_x}} \nabla_{s_{x_{t_x}}} f(s_{x_{t_x}}) \cdot f(s_{y_0})$ 
4:    $s_{x_{t_x-1}} := \sqrt{\bar{\alpha}_{t_x-1}} \left( \frac{s_{x_{t_x}} - \sqrt{1 - \bar{\alpha}_{t_x}} \hat{\epsilon}_\theta^x(s_{x_{t_x}}, s_{y_0}, t_x, t_y = 0)}{\sqrt{\bar{\alpha}_{t_x}}} \right) + \sqrt{1 - \bar{\alpha}_{t_x-1}}$ 
5: end for
6: return  $s_{x_0}$ 

```

5 Evaluation

5.1 Dataset

We collected a proprietary speech and text dataset from the Kenya Broadcasting Corporation (KBC), which operates 11 radio stations broadcasting in both English and various Kenyan vernacular languages. News articles originally written in English were translated into these vernacular languages and read by presenters at different times throughout the day. This process allowed us to gather news articles in English, their corresponding translations into local languages, and the associated speech recordings. The news articles presented across different vernacular stations during the same time slots maintained the same semantic content, ensuring consistency across translations.

The news articles were delivered by multiple newscasters, introducing diversity in speech patterns, accents, and vocal styles, which enriches the dataset by exposing models to a wide range of speaking styles. This variation in speech enhances the dataset’s utility for tasks involving speaker variation, making it valuable for speech recognition and speech-to-speech translation systems.

We focused on the 7 pm news bulletins, which represent the most comprehensive broadcasts, consolidating the day’s news. The dataset consists of news bulletins aired between 2018 and 2023. To ensure consistency in semantic content, the speech data was pre-processed to remove advertisements, which varied across radio stations.

From the 11 languages available, we selected five of the most widely spoken languages in Kenya: Swahili, Luo, Kikuyu, Nandi, and English. These languages were chosen based on their prevalence and cultural significance in Kenya, representing the major linguistic groups in the country. Details of the pre-processed dataset are provided in Table 3.

Table 1: Summary of speech dataset used for evaluation.

Language	Phylum	No. of news bulletins collected	Total length of speech (hrs)
Swahili	Niger-Congo	2190	1353
Luo	Nilo-Saharan	2190	1284
Kikuyu	Niger-Congo	2190	1304
Nandi	Nilo-Saharan	2190	1256
English	-	2190	1206

The dataset provides a rich resource for studying linguistic diversity and translation consistency across languages from different language families (Niger-Congo, Nilo-Saharan, and English as a global language). The pre-processing ensured that each speech segment retained semantic fidelity while removing inconsistencies like advertisements and other non-relevant audio. Furthermore, the presence of multiple speakers within each language adds an additional layer of complexity and realism to the dataset, making it suitable for tasks such as automatic speech recognition (ASR), speech synthesis, and speech-to-speech translation (S2ST).

5.2 Segment generation

The news bulletins in the languages listed in Table 1 were segmented using the technique described in Section 4.1. Table 2 provides a summary of the average segment length and the total number of segments generated for each language.

Table 2: Segment generation statistics for the speech dataset.

Language	Average Segment Length (l) (s)	Total No. of Segments Generated
Luo	16.5	601,112
Nandi	17.1	594,503
Kikuyu	15.6	643,001
English	15.0	665,578
Swahili	15.2	638,944

From the segmentation analysis, we observe that languages within the same phylum tend to generate segments with smaller deviations in their average lengths. For example, the difference in average segment length between Nandi and Luo (both Nilo-Saharan languages) is 0.6 seconds, while the difference between Kikuyu and Swahili (both Niger-Congo languages) is 0.4 seconds. In contrast, Luo and Kikuyu, which belong to different phyla, show a larger deviation of 0.9 seconds. For these pilot languages, the trend suggests that linguistic similarities within a phylum may influence the segmentation process, affecting both the average segment length and the total number of segments generated.

5.3 Segment pairing

We paired segments from two languages both within a phylum and across two different phyla. We specifically paired Luo-Nandi segments (same phylum), Luo-Kikuyu (cross-phyla), Kikuyu-Swahili (same phylum), Swahili-English and Luo-English. To pair the segments we used the technique described in section 4.2. The number of pairs generated for each paired languages shown in Table 3.

Table 3: Summary of pairs generated between languages

Language pair	No. of pairs generated
Luo-Nandi(target)	589,637
Luo-Kikuyu(target)	632,102
Kikuyu-Swahili(target)	612,645
Swahili-English(target)	765,944
Luo-English(target)	778,456

5.4 Segment encoder training

We trained a global segment encoder model, f_s , using a contrastive learning approach to embed paired speech segments from different languages. The training dataset consisted of 70% of the paired segments from each language pair, as shown in Table 3.

The training process involved both clean and noised segments. Specifically, we introduced noise to half of the training segments by sampling a noise value ϵ^x from a standard Gaussian distribution and adding it to the latent representation of a randomly selected segment s_x from a given language x . The other half of the training data consisted of clean, unaltered segments. This mixture allowed the model to generalize well across both clean and noisy speech conditions.

The model was trained with a contrastive learning objective. During training, segments from the same language were considered positive pairs, encouraging their embeddings to be similar in the latent space, while segments from different languages were treated as negative pairs, encouraging their embeddings to be more distinct. To ensure consistency across the dataset, all speech segments were padded to match the length of the largest segment, which was 20 seconds. This uniform padding ensured that all input data had the same dimensions, facilitating efficient batch processing during training.

The segment encoder was pre-trained over 1 million steps, with a batch size of 512. We employed the AdamW optimizer with hyperparameters $\beta_1 = 0.9$, $\beta_2 = 0.98$, and $\epsilon = 10^{-9}$ to stabilize the training process and prevent overfitting.

Further, the learning rate was initialized to 1×10^{-4} and reduced progressively using a cosine annealing schedule, which helped optimize the convergence of the model. Regular checkpoints were saved during training to evaluate the model’s performance on the validation set, ensuring that we maintained the best-performing version of the encoder.

5.5 Sentence pairing

For each speech collected, we used the corresponding news article that was read as the ground truth reference text. To create parallel text datasets, we manually paired sentences from the collected news articles. The pairing process aimed to match semantically similar sentences across the five languages shown in Table 3. This resulted in five sets of parallel text datasets, one for each pair of languages.

The manual pairing process was guided by semantic similarity, ensuring that the sentences conveyed the same meaning across languages. These parallel datasets are crucial for evaluating translation performance and for training language models on semantically aligned data.

5.6 Automatic Segment Pairing Accuracy Evaluation

We pre-trained five language-specific ASR models to generate text from the corresponding speech in any of the five languages listed in Table 4. For the Nandi, Kikuyu, and Luo languages, we used the Squeezeformer model Kim et al. (2022), while for Swahili and English, we fine-tuned the Whisper small model Radford et al. (2023). Table 4 reports the word error rates (WER) of these pre-trained ASRs.

Table 4: ASR’s WER values for different languages.

Language	WER (%)
Nandi	13.6
Luo	14.2
Kikuyu	14.4
Swahili	9.8
English	5.3

We also trained machine translation (MT) models using the original transformer (base) configuration. The MT models were trained using the number of paired sentences listed in Table 5. The BLEU scores for each language pair on the test dataset are also provided.

Table 5: Number of paired sentences used for training MT models and BLEU scores.

Language Pair	Paired Sentences	BLEU Score
Luo-Nandi	1.76M	28.6
Luo-Kikuyu	1.18M	31.2
Kikuyu-Swahili	1.29M	30.4
Swahili-English	1.52M	35.4
Luo-English	1.34M	31.7

Evaluating the accuracy of the segment pairing technique, where given a pair of segments (s_x, s_y) , would typically require substantial human effort. Human evaluators would need to listen to both the source segment s_y and the target segment s_x , then evaluate their pairing accuracy based on predefined criteria Duquenne et al. (2021). However, this method is costly and time-consuming.

To address this challenge, we implemented two automated, indirect methods to evaluate segment pairing:

- **Method 1: ASR + MT:** The source speech segment s_y is first transcribed using an ASR model, producing the text transcription \hat{t}_y . This transcription is then passed to a machine translation (MT) model, which translates it into the target language, producing the estimated target text \hat{t}_x^{MT} . To evaluate the accuracy of this translation, we compare \hat{t}_x^{MT} to the reference transcription t_x^{ASR} , which is the transcription of the target speech segment s_x , using a BLEU score Papineni et al. (2002).
- **Method 2: ASR + Search:** To reduce errors introduced by ASR and MT models, once the MT output \hat{t}_x^{MT} is generated, we perform a search on the target language reference text to find the sentence t_x^{MT} that best matches the MT output. Similarly, the target speech segment s_x is ASR-transcribed to generate another text output \hat{t}_x^{ASR} . We then perform a search for the closest match in the target reference text to extract the corresponding t_x^{ASR} for the ASR output. Finally, we compute the BLEU score between t_x^{MT} and t_x^{ASR} to assess the similarity of the two matched sentences.

After computing BLEU scores, precision (p), recall (r), and F-measure (f) are calculated based on these scores. A BLEU score threshold of 23.4 is used to categorize segment pairs as correctly paired.

$$p = \frac{\text{Number of correctly paired segments between languages } x \text{ and } y}{\text{Total number of paired segments between } x \text{ and } y}$$

$$r = \frac{\text{Number of correctly paired segments between languages } x \text{ and } y}{\text{Total number of segments in the target language } x}$$

$$f = 2 \times \frac{p \times r}{p + r}$$

Figure 3 shows the precision, recall, and F-measure values for segment pairing between different language pairs. Two key observations can be drawn:

1. **Phylum Influence:** The pilot dataset suggests that the segment pairing technique performs better when both languages belong to the same phylum. For example, as shown in Figure 3, the precision, recall, and F-measure for Luo-Nandi (same phylum) are significantly higher than for Luo-Kikuyu (different phylum), indicating that phylum classification may contribute to improved pairing accuracy.
2. **Impact of MT and ASR Errors:** MT and ASR errors significantly affect segment pairing accuracy. When MT and ASR sentences are directly compared, the precision, recall, and F-measure for Luo-Nandi are 67.32%, 65.44%, and 66.37%, respectively. However, replacing MT and ASR-generated sentences with search-matched sentences improved these metrics to 70.01%, 68.21%, and 69.10%, respectively.

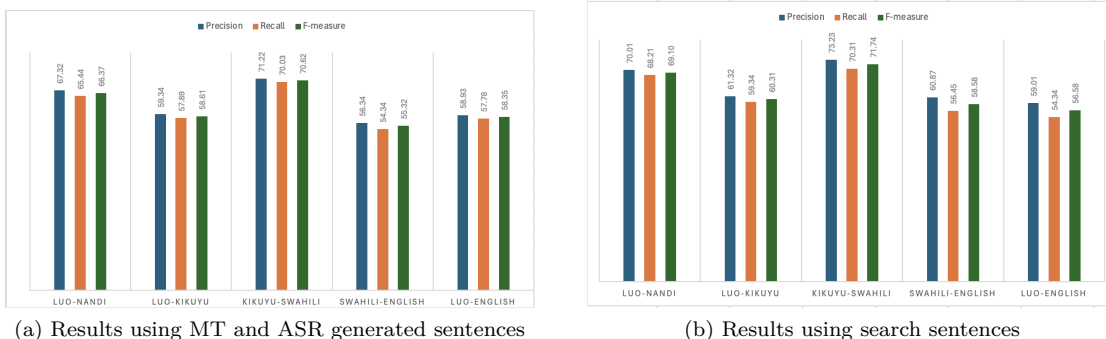


Figure 3: Precision, recall, and F-measure values for segment pairing across different language pairs. (a) Results using MT model; (b) Results using search-generated sentences.

5.7 Manual Segment pairing evaluation

For manual segment pairing evaluation, we recruited undergraduate students who were native speakers of Nandi, Luo, and Kikuyu—the primary languages used in this study. The students were selected from a pool of BSc students who responded to an advertisement posted on a notice board. A total of 2,367 students volunteered, and all of them were included in the study. Each student received a token payment of Ksh 200 for their transcription work.

All participants were proficient in both English and Swahili, making them well-suited for accurately transcribing the speech data. For each language pair listed in Table 3, we randomly selected 1,000 segment pairs. Each student was tasked with listening to a segment in their native language and transcribing it into English, which served as the common reference language for comparison.

Each student was assigned 20 segments and was required to provide both the segment number and its transcription. For each segment pair (s_x, s_y) , the segment s_x was given to a student proficient in language x , while the segment s_y was assigned to a student proficient in language y . Both students transcribed their respective segments into English.

To ensure transcription accuracy, each segment s_x was transcribed by at least two students. Additionally, two independent evaluators (verifiers) compared the transcriptions of the same segment for similarity. The verifiers used a scale from 1 to 5, where 5 represented complete similarity, to rate the consistency between the two transcriptions. If the similarity score between any two transcriptions for a given segment was 4 or higher, the transcription was considered accurate.

We used BLEU scores to compute precision, recall, and F-measure as described in Section 4.7. Figure 4 reports the results.

Finally, we computed BLEU scores between the verified transcriptions of segment s_x and segment s_y to evaluate the semantic alignment of paired segments across languages. A higher BLEU score indicated stronger semantic alignment, allowing us to quantitatively assess the effectiveness of our segment pairing method.

The results of the manual evaluation show a similar trend to that of the automatic evaluation, where the location-based segment pairing technique performs better when the two languages are from the same phylum. For example, the manual evaluation for Luo-Nandi (same phylum) achieved precision, recall, and F-measure scores of 66.4%, 63.8%, and 65.1%, respectively. This closely aligns with the results obtained from the automatic ASR + Search method, which yielded precision, recall, and F-measure scores of 67.32%, 65.44%, and 66.37%, respectively.

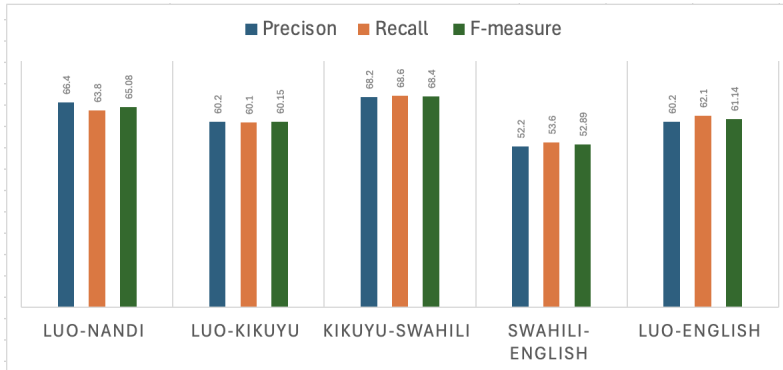


Figure 4: Precision, recall, and f-measure values for segment pairing across different language pairs using manual technique

6 Effect of Segment Length on Segment Mapping Quality

In this section, we investigate how segment length impacts the quality of segment pairing. We categorized a segment pair as long if both segments of the pair are longer than the average segment length l_x for language x , as defined in Table 2. A segment pair was categorized as short if both segments were shorter than l_x , and as average length if both segments in the pair were approximately equal to l_x .

To evaluate the effect of segment length, we randomly selected 1000 short, average, and long segment pairs from three language pairings: Luo-Nandi, Luo-Kikuyu, and Kikuyu-Swahili. We used the **Method 2: ASR + Search** technique to evaluate the quality of the segment matches for each category.

Figure 5 summarizes the results, showing that segment pairs of average length consistently achieve the highest pairing quality, with the lowest variability across all three language pairings. Short segments also performed relatively well but exhibited slightly more variability. Long segment pairs demonstrated the lowest pairing quality and the highest variability, suggesting that longer segments are more prone to quality degradation during the pairing process.

This analysis indicates that as segment length increases, the likelihood of a drop in pairing quality also increases. Upon Manual investigation on why the quality of long segment pairings was lower, we found that many paired long segments contained uneven spillover sentences. In these cases, both segments included a complete sentence and half of another sentence, but the segments did not end at the same time. This discrepancy introduced errors in the pairing process, reducing the overall quality.

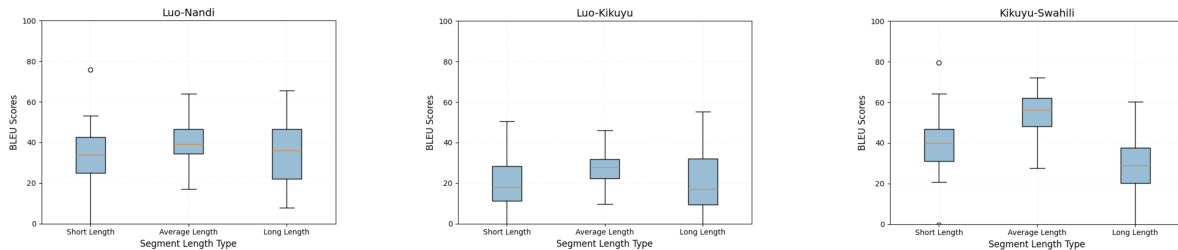


Figure 5: Effect of segment length on pairing quality for the Luo-Nandi, Luo-Kikuyu, and Kikuyu-Swahili pairings.

6.1 Diffusion Model Training

To optimize translation accuracy between language pairs, we trained five unified diffusion models, each specifically for a unique language pair listed in Table 3, as illustrated in Figure 3. These models, collectively referred to as the **Segment-Aware Unified Diffusion Model (SegUniDiff)**, were trained using 70% of

the total segment pairs for each language combination (the same segments utilized in training the segment encoder f_s). Each segment in the training dataset was padded to a uniform length of 20 seconds to ensure consistency across inputs.

Each segment s_x was encoded by the speech encoder to produce a representation $s_{x_{t_0}} \in \mathbb{R}^{F \times T}$, where F denotes frequency bins and T denotes time steps. This encoded representation $s_{x_{t_0}}$ was then subjected to a forward diffusion process with $N = 1000$ steps. We applied a constant noise variance, increasing linearly from α_1 to α_T , using a noise schedule defined by $Linear(1 \times 10^{-4}, 0.005, 1000)$ for controlled degradation.

Subsequently, the noised segment $s_{x_{t_x}} \in \mathbb{R}^{F \times T}$ was divided into overlapping chunks along the time axis, with each chunk of length L overlapping by 50%. This process produced the final input $s'_{x_{t_x}} \in \mathbb{R}^{F \times L \times N}$, which was then passed to the transformer-based noise prediction model.

For conditioning, we used a mel-spectrogram c generated from the original speech signal. The signal was downsampled to 24 kHz, with 128-dimensional mel-spectrogram features extracted using a 50 ms Hanning window, a 12.5 ms frame shift, and a 2048-point FFT, with frequency cutoffs at 20 Hz and 12 kHz.

Each model was trained for 1 million steps on a single V100 GPU, utilizing the AdamW optimizer with parameters $\beta_1 = 0.9$, $\beta_2 = 0.98$, and $\epsilon = 10^{-9}$.

6.2 Translation Accuracy Evaluation

To evaluate translation accuracy, we performed both unconditional and conditional predictions on pairs of segments (s_x, s_y) in the test dataset. First, an unconditional prediction of \hat{s}_x was generated using inputs $s_{x_{t_T}}$ and $s_{y_{t_T}}$, denoted by $\epsilon_{\theta}^x(s_{x_{t_T}}, s_{y_{t_T}}, t_T, t_T)$ (see Algorithm 1 for details). For the conditional prediction $\hat{s}_x | s_y$, we provided $s_{x_{t_T}}$ and $s_{y_{t_0}}$ as input, represented by $\epsilon_{\theta}^x(s_{x_{t_T}}, s_{y_{t_0}}, t_T, t_0)$ (see Algorithm 3).

Next, to evaluate translation accuracy, we transcribed the source segment s_y using an Automatic Speech Recognition (ASR) model, generating \hat{t}_y . A search was conducted in the source language reference text to identify the sentence t_y most closely matching \hat{t}_y . From the corresponding paired sentence set, the translated target text t_x^{ref} was chosen as the reference. The estimated target speech \hat{s}_x was then transcribed using the ASR model for the target language to yield \hat{t}_x^{ASR} , and the BLEU score between \hat{t}_x^{ASR} and t_x^{ref} was calculated to assess translation accuracy.

Table 6: BLEU scores for different configurations of the proposed S2ST technique.

Conditional	Unconditional	Noised target segments	Clean target segments	Luo-Nandi	Luo-Kikuyu	Kikuyu-Swahili	Swahili-English	Luo-English
✗	✓	✓	✗	27.4	20.5	30.3	23.3	19.4
✗	✓	✗	✓	23.3	21.5	24.5	20.3	18.8
✓	✗	✓	✗	35.6	26.1	36.8	25.4	23.3
✓	✗	✗	✓	31.5	23.2	32.9	23.7	20.4
Cascaded (ASR → MT → TTS)	✗	✗	✗	37.5	37.2	40.9	40.1	39.4
Cascaded (ASR → Search → TTS)	✗	✗	✗	38.2	39.7	42.3	41.4	41.2

The following key observations were made:

1. Translation quality is higher when the pseudo-classifier composed of noised target segments is used to guide the translation.
2. Translation quality improves when language pairs belong to the same phylum.
3. The best translation results are achieved when the conditional model is used in combination with a pseudo-classifier with noised target segments.
4. The cascaded approach (ASR → MT → TTS) significantly outperforms the proposed S2ST technique.

7 Speech Translation Generation

We evaluated the efficiency of the speech translation process by measuring the time taken by the model to generate a single n -frame speech sample. The reported translation speed represents the average time per speech sample across the entire test dataset. To standardize the evaluation, we down-sampled the target segment s_{x_0} to 24 kHz and extracted 128-dimensional mel-spectrogram features using a 50 ms Hanning window, a 12.5 ms frame shift, and a 2048-point FFT.

The latency analysis was conducted on a V100 GPU, and the results are illustrated in Figure 6. The proposed guided diffusion technique, evaluated in both unconditional and conditional settings, demonstrated a nearly constant translation speed across different input configurations. This stands in contrast to the cascaded approach, which exhibited a linear increase in translation time as the number of frames in the input segment grew.

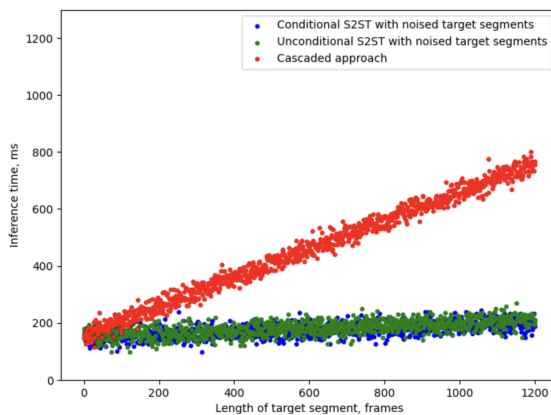


Figure 6: Translation speed for different configurations.

As shown in Figure 6, the guided diffusion model outperforms the cascaded approach, particularly for longer speech samples, where the cascaded approach’s translation speed degrades linearly with increasing input size. This highlights the guided diffusion method’s scalability and efficiency, especially when dealing with larger speech inputs.

8 Limitation of study

- **Dataset Specificity:** The dataset used in this study originates from news broadcasts, characterized by formal language, clear pronunciation, and controlled acoustic environments. While this dataset is suitable for initial evaluation, it may not capture the diversity and complexity of everyday conversational speech, which includes spontaneous language and varied acoustic conditions. Evaluating the model’s performance on more diverse datasets, especially those with conversational speech and challenging acoustic conditions, would be necessary to establish its robustness and generalizability.
- **Limited Language Selection:** This study focuses on a specific set of Kenyan languages, allowing an exploration of linguistic similarities within a closely related group potentially influenced by geographical proximity. Expanding to languages from varied geographical regions and language families would provide insight into the broader applicability of this approach.

9 Conclusion

This work investigates how similarity within African languages grouped within a phylum can be exploited to achieve direct S2ST. We implement a segment-based translation using guided diffusion. We evaluate the developed model using different language pairs of speeches. The speeches are paired both within a phylum and across a phylum. The evaluation results show that when languages have close linguistic speech properties

segment-based translation is a viable technique. This can be used when data annotation is impossible or expensive the need for data annotation.

References

- Fan Bao, Shen Nie, Kaiwen Xue, Chongxuan Li, Shi Pu, Yaole Wang, Gang Yue, Yue Cao, Hang Su, and Jun Zhu. One transformer fits all distributions in multi-modal diffusion at scale. In *International Conference on Machine Learning*, pp. 1692–1717. PMLR, 2023.
- Loïc Barrault, Yu-An Chung, Mariano Coria Meglioli, David Dale, Ning Dong, Paul-Ambroise Duquenne, Hady Elsahar, Hongyu Gong, Kevin Heffernan, John Hoffman, et al. Seamless4t-massively multilingual & multimodal machine translation. *arXiv preprint arXiv:2308.11596*, 2023a.
- Loïc Barrault, Yu-An Chung, Mariano Coria Meglioli, David Dale, Ning Dong, Mark Duppenhaler, Paul-Ambroise Duquenne, Brian Ellis, Hady Elsahar, Justin Haaheim, et al. Seamless: Multilingual expressive and streaming speech translation. *arXiv preprint arXiv:2312.05187*, 2023b.
- Ting Chen, Simon Kornblith, Mohammad Norouzi, and Geoffrey Hinton. A simple framework for contrastive learning of visual representations. In *International conference on machine learning*, pp. 1597–1607. PMLR, 2020.
- G Tucker Childs. An introduction to african languages. *An Introduction to African Languages*, pp. 1–285, 2003.
- Paul-Ambroise Duquenne, Hongyu Gong, and Holger Schwenk. Multimodal and multilingual embeddings for large-scale speech mining. *Advances in Neural Information Processing Systems*, 34:15748–15761, 2021.
- Zygmunt Frajzyngier. Afroasiatic languages. In *Oxford Research Encyclopedia of Linguistics*. 2018.
- Marco Gaido, Matteo Negri, Mauro Cettolo, and Marco Turchi. Beyond voice activity detection: Hybrid audio segmentation for direct speech translation. *arXiv preprint arXiv:2104.11710*, 2021.
- Jonathan Ho, Ajay Jain, and Pieter Abbeel. Denoising diffusion probabilistic models. *Advances in neural information processing systems*, 33:6840–6851, 2020.
- Rongjie Huang, Jinglin Liu, Huadai Liu, Yi Ren, Lichao Zhang, Jinzheng He, and Zhou Zhao. Transpeech: Speech-to-speech translation with bilateral perturbation. *arXiv preprint arXiv:2205.12523*, 2022.
- Ye Jia, Ron J Weiss, Fadi Biadsy, Wolfgang Macherey, Melvin Johnson, Zhifeng Chen, and Yonghui Wu. Direct speech-to-speech translation with a sequence-to-sequence model. *arXiv preprint arXiv:1904.06037*, 2019.
- Ye Jia, Michelle Tadmor Ramanovich, Tal Remez, and Roi Pomerantz. Translatotron 2: High-quality direct speech-to-speech translation with voice preservation. *arXiv preprint arXiv:2107.08661*, 2021.
- Sehoon Kim, Amir Gholami, Albert Shaw, Nicholas Lee, Karttikeya Mangalam, Jitendra Malik, Michael W Mahoney, and Kurt Keutzer. Squeezeformer: An efficient transformer for automatic speech recognition. *Advances in Neural Information Processing Systems*, 35:9361–9373, 2022.
- Ann Lee, Peng-Jen Chen, Changhan Wang, Jiatao Gu, Sravya Popuri, Xutai Ma, Adam Polyak, Yossi Adi, Qing He, Yun Tang, et al. Direct speech-to-speech translation with discrete units. *arXiv preprint arXiv:2107.05604*, 2021.
- Evgeny Matusov, Stephan Kanthak, and Hermann Ney. On the integration of speech recognition and statistical machine translation. In *Ninth European Conference on Speech Communication and Technology*, 2005.
- Hermann Ney. Speech translation: Coupling of recognition and translation. In *1999 IEEE International Conference on Acoustics, Speech, and Signal Processing. Proceedings. ICASSP99 (Cat. No. 99CH36258)*, volume 1, pp. 517–520. IEEE, 1999.

-
- Alex Nichol, Prafulla Dhariwal, Aditya Ramesh, Pranav Shyam, Pamela Mishkin, Bob McGrew, Ilya Sutskever, and Mark Chen. Glide: Towards photorealistic image generation and editing with text-guided diffusion models. *arXiv preprint arXiv:2112.10741*, 2021.
- Kishore Papineni, Salim Roukos, Todd Ward, and Wei-Jing Zhu. Bleu: a method for automatic evaluation of machine translation. In *Proceedings of the 40th annual meeting of the Association for Computational Linguistics*, pp. 311–318, 2002.
- Tomasz Potapczyk and Pawel Przybysz. Srpol’s system for the iwslt 2020 end-to-end speech translation task. In *Proceedings of the 17th International Conference on Spoken Language Translation*, pp. 89–94, 2020.
- Alec Radford, Jong Wook Kim, Chris Hallacy, Aditya Ramesh, Gabriel Goh, Sandhini Agarwal, Girish Sastry, Amanda Askell, Pamela Mishkin, Jack Clark, et al. Learning transferable visual models from natural language supervision. In *International conference on machine learning*, pp. 8748–8763. PMLR, 2021.
- Alec Radford, Jong Wook Kim, Tao Xu, Greg Brockman, Christine McLeavey, and Ilya Sutskever. Robust speech recognition via large-scale weak supervision. In *International Conference on Machine Learning*, pp. 28492–28518. PMLR, 2023.
- Björn Schuller, Stefan Steidl, Anton Batliner, Felix Burkhardt, Laurence Devillers, Christian Müller, and Shrikanth Narayanan. Paralinguistics in speech and language—state-of-the-art and the challenge. *Computer Speech & Language*, 27(1):4–39, 2013.
- Jiaming Song, Chenlin Meng, and Stefano Ermon. Denoising diffusion implicit models. *arXiv preprint arXiv:2010.02502*, 2020.
- Mingxing Tan and Quoc Le. Efficientnet: Rethinking model scaling for convolutional neural networks. In *International conference on machine learning*, pp. 6105–6114. PMLR, 2019.
- Enrique Vidal. Finite-state speech-to-speech translation. In *1997 IEEE International Conference on Acoustics, Speech, and Signal Processing*, volume 1, pp. 111–114. IEEE, 1997.
- Chen Zhang, Xu Tan, Yi Ren, Tao Qin, Kejun Zhang, and Tie-Yan Liu. Uwspeech: Speech to speech translation for unwritten languages. In *Proceedings of the AAAI Conference on Artificial Intelligence*, volume 35, pp. 14319–14327, 2021.

A Model Specifications

The model used is a transformer-based architecture designed for speech-to-speech translation (S2ST). It comprises multi-head attention layers, feedforward layers, and multi-layer perceptrons (MLP). The model has 8 attention heads, 8 layers for depth, a feedforward layer size of 1024, and an MLP with 2045 dimensions. These settings balance computational efficiency and performance.

Table 7: Model specifications used for evaluation.

Heads	Layers	Feedforward Size (FFW)	MLP
8	8	1024	2045